THE JOURNAL OF BIOLOGICAL CHEMISTRY VOL. 285, NO. 30, pp. 23477–23485, July 23, 2010

A Systems Biology Approach to Dissection of the Effects of Small Bicyclic Peptidomimetics on a Panel of *Saccharomyces cerevisiae* Mutants*[S]

Received for publication, March 19, 2010, and in revised form, May 24, 2010 Published, JBC Papers in Press, May 25, 2010, DOI 10.1074/jbc.M110.125153

Irene Stefanini[‡], Andrea Trabocchi[§1], Emmanuela Marchi[‡], Antonio Guarna[§], and Duccio Cavalieri[‡2]

From the [‡]Department of Pharmacology "Mario Aiazzi Mancini" and the [§]Department of Chemistry "Ugo Schiff," University of Florence, 50139 Florence, Italy

In recent years, an approach called "chemical genetics" has been adopted in drug research to discover and validate new targets and to identify and optimize leads by high throughput screening. In this work, we tested the ability of a library of small peptidomimetics to induce phenotypic effects with functional implications on a panel of strains of the budding yeast *Saccharomyces cerevisiae*, both wild type and mutants, for respiratory function and multidrug resistance. Further elucidation of the function of these peptidomimetics was assessed by testing the effects of the compound with the most prominent inhibitory activity, 089, on gene expression using DNA microarrays. Pathway analysis showed the involvement of such a molecule in inducing oxidative damage through alterations in mitochondrial functions. Transcriptional experiments were confirmed by increased levels of ROS and activation of mitochondrial membrane potential. Our results demonstrate the influence of a functional *HAP1* gene in the performance of *S. cerevisiae* as a model system.

Pharmaceutical and biotechnological fields are constantly looking for new drugs characterized by innovation and economy (1). New approaches emerging from chemical and biological knowledge, such as "chemical genetics" (2), consist of the study of biological systems by systematic investigation of the effects of small molecules on a specific cellular model rather than perturbing with gene mutations (3–5). This new approach has been divided into forward and reverse chemical genetics; the former is based on the research of a desired phenotypic effect following the administration of small molecules to biological systems of interest, whereas the latter is based on the investigation of the effects of small molecules against a specific target (6–8). To make these new approaches time- and money-saving, the set-up of easy, rapid, and economical chemical synthesis and biological screening processes is essential (9, 10). The budding yeast *Saccharomyces cerevisiae*, which has been defined as an "honorary mammal" (11), is a suitable model organism for this aim, mainly because of the high degree of conservation with human cells concerning main biological processes (11). Thanks to its ease of manipulation, it can be successfully used to identify molecules of pharmacological interest (4, 12). Moreover, once active compounds have been selected, functional information about their mode of action can be inferred from screening ~5000 viable yeast haploid deletion mutant strains for hypersensitivity or hyperresistance to each molecule, thus identifying pathways that influence the cellular response to tested compounds (13–16). However, so far, chemical genetic approaches have used only one genetic background, that of laboratory strain S288c, which is limited by an accumulation of genetic defects, such as the inability to sustain proper respiratory metabolism of this strain (4, 17–19). In this work, we selected a panel of strains in which it is possible to investigate the influence of a library of molecules on growth rate, respiratory metabolism (*HAP1*), and multidrug-membrane function (*ERG6*, *SNQ2*, and *PDR3*).

Peptidomimetics (20) play a prominent role as candidate compounds to induce phenotypic effects on biological systems. In fact, side-chain recognition dominates biological interactions of almost all cellular processes; thus, peptidomimetics, initially developed for their property of preventing degradation and improving oral bioavailability of peptide-based drugs, have been envisaged as a tool for perturbing such interactions and identifying protein function. Small peptide-based agents have attracted wide interest as cancer-targeting and anti-infective agents, and there is a need to develop new high affinity and high specificity peptidomimetic or small molecule ligands in such widespread pathologies. Success in this area depends on the ability to create novel complex molecular structures of a peptidomimetic nature as tools for probing protein-protein interactions. Diversity-oriented synthesis (21) is the concept of choice for the rapid exploration of the chemical space. Our efforts are oriented to the development of efficient synthetic strategies for the production of rigid and polyfunctional heterocyclic templates using elements from the chiral pool, such as carbohydrates and amino acids, which guarantee a high stereochemical and functional diversity (22–26). The library of small peptidomimetics herein taken into account was synthesized by focusing on a

* This work was supported by Network of Excellence in Nutrigenomics (NuGO) Grant FOOD-CT-2004-506360, European Union Grant LSHB-CT-2004-512074, the Network of Excellence DC-THERA (Dendritic Cells for Novel Immunotherapies), SYBARIS Grant Agreement 242220, Fondazione Roma, Consorzio Interuniversitario Nazionale "Metodologie e Processi Innovativi di Sintesi" and Ministero dell'Istruzione, dell'Università e della Ricerca Programmi di ricerca di Rilevante Interesse Nazionale Grant 519MIUR060.

[S] The on-line version of this article (available at http://www.jbc.org) contains supplemental Tables 1 and 2 and Fig. 1.

The gene expression and hybridization array data can be accessed through the NCBI repository, GEO, under NCBI accession number GSE19331.

[1] To whom correspondence may be addressed: Via della Lastruccia 13, 50019 Florence, Italy. Fax: 39-0554573531; E-mail: andrea.trabocchi@unifi.it.

[2] To whom correspondence may be addressed: Viale Pieraccini 6, 50139 Florence, Italy. Fax: 390554271280; E-mail: duccio.cavalieri@unifi.it.

bicyclic scaffold based on the 6,8-dioxa-3-azabicyclo[3.2.1]octane core and diverse substituents, in order to hypothesize a connection between specific groups and biological effects.

EXPERIMENTAL PROCEDURES

Molecules—In this study, a preconstituted library, composed of bicyclic peptidomimetics, bicycles from tartaric acid and amino acids (BTAa),[3] was used for assays on selected yeast strains (supplemental Table 1).

Yeast Strains and Media—Three wild-type strains were used: W303 (*MATα can1-100 ade2-1 his3-11,15 leu2-3,112 trp1-1, ura3-1*), BY4742 (*MATα his3 leu2 lys2 ura3*), and 0117. The deletion strains used were BY4742Δ*snq2* (*MATα his3 leu2 lys2 ura3 snq2*::*kanMX*), BY4742Δ*pdr3* (*MATα his3 leu2 lys2 ura3 pdr3*::*kanMX4*), and BY4742Δ*erg6* (*MATα his3 leu2 lys2 ura3 erg6*::*kanMX4*). Yeast strains used to simulate the *HAP1* pattern of BY4742 were FY2607 (*MATa ura3 his3 leu2 lys2-128^{TM} hap1T*), FY2609 (*MATa ura3 his3 leu2 lys2-128^{TM}*) and FY2611 (*MATa ura3 his3 leu2 lys2-128^{TM} hap1*:*kanMX4*). For growth inhibition tests, yeast cells were inoculated at 1×10^5 cells/ml in YPD medium (yeast peptone dextrose, yeast extract 1% (w/v), peptone 2% (w/v), buffered at pH 4.8 with acetic acid, 2% glucose).

First Level Assays—First level assays allowed the selection of a restricted number of active molecules. W303 and 0117 strains were grown in YPD. The different cultures were dispensed at equal volume onto 96-well plates, each well containing a different compound at a concentration of 0.1 mM. The assay plates were incubated at 28 °C with shaking, and yeast growth was scored by measurement of A_{650} with a Victor high throughput microplate spectrophotometer equipped with a 96-well plate reader (PerkinElmer Life Sciences) every 2 h for the first 24 h and then once a day for 7 days. Compounds responsible for the variation in cell growth during the exponential phase or in the OD_{650} value of the stationary phase or both were selected for further characterization. These compounds were tested at concentrations of 1, 0.5, 0.4, 0.3, 0.2, and 0.1 mM.

Second Level Assays—Second level assays were carried out to give more insight into the results obtained from the first run of assays. Molecules selected because of their significant effects on the wild-type strains at the concentration of 0.3 mM were tested on BY4742Δ*erg6*, BY4742Δ*snq2*, and BY4742Δ*pdr3* strains. Strains were grown in YPD supplemented with the molecule at 0.3 mM concentration and monitored with the same protocol applied in the first level assay.

Normalization of OD_{650} Values—The OD_{650} values used to define the growth curves were evaluated as the difference between OD_{650} at t_x and OD_{650} at t_0. The percentage effect of each molecule (% effect) was calculated as a function of the OD_{650} value of treated cells in the stationary phase ($OD_{650}^{st.ph.treat}$) and the OD_{650} of untreated cells in the stationary phase ($OD_{650}^{st.ph.ctrl}$).

$$\%\ \text{effect} = \frac{OD_{650}^{st.ph.treat} - OD_{650}^{st.ph.ctrl}}{OD_{650}^{st.ph.ctrl}} \times 100 \qquad \text{(Eq. 1)}$$

Determination of the Minimum Inhibitory Concentration (MIC)—Wild-type strains (W303 and BY4742) were grown in 2 ml of YPD (pH 4.8) supplemented with the most active compound, **089** ((7*R*)-3-benzhydryl-2-oxo-5-phenyl-6,8-dioxa-3-aza-bicycle[3.2.1]octane-7-carboxyl-ethylamide), at concentrations of 1, 0.5, 0.4, 0.3, 0.2, and 0.1 mM. The assay cultures were incubated at 28 °C with shaking. After 3 days, the concentration of the cells was determined, and 100 cells were plated (100 cells/plate) on YPD agar (in two replicates). After 5 days, colony-forming units were calculated, and the concentration-effect curve of the treatment was plotted.

Determination of Survival Rate—This test was carried out with the LIVE/DEAD® yeast viability assay (Molecular Probes), following the manufacturer's instructions, and with the methylene blue assay determining the survival rate of the two wild-type W303 and BY4742 strains and of the BY4742Δ*erg6*, BY4742Δ*snq2*, and BY4742Δ*pdr3* strains. Cells were grown in YPD supplemented with **089** at concentrations of 1, 0.5, 0.4, 0.2, and 0.1 mM; a positive control was also carried out without the compound. The assay cultures were incubated at 28 °C, and after 2 and 4 h, aliquots were processed with the LIVE/DEAD and methylene blue assays, permitting calculation of the survival rate (number of live cells counted × 100/total number of cells in the positive control culture).

Microarray Hybridization—Yeast microarrays were constructed as described previously (27). Yeast cells (BY4742, BY4742Δ*erg6*, and BY4742Δ*snq2* strains) were treated in YPD (pH 4.8) supplemented with **089** at 0.2 mM concentration and incubated at 28 °C with shaking for 4 h. RNA was extracted from about 1×10^9 cells using the hot acid phenol/chloroform protocol. RNAs were quantified spectrophotometrically using Nanodrop and by measuring the absorbance at 230, 260, and 280 nm and then calculating the 260/230 and 260/280 ratios and considering good data to be values of 1.8–2.2. RNA integrity was checked by electrophoresis in 1% agarose gel stained with ethidium bromide. RNAs from cells treated with **089** (labeled with Cy5) were compared with RNAs from cells grown in YPD as the reference sample (labeled with Cy3) (CyDye Mono-Reactive Dye Pack, Amersham Biosciences). The labeling method used was the indirect method described by DeRisi (see the University of California San Francisco DeRisi laboratory Web site). Hybridization took place at 63 °C for 14–16 h.

Gene Expression Analysis—Fluorescent cDNA bound to the microarray was detected with a GenePix 4000B microarray scanner (Axon Instruments), using the GenePixPro6.1 software package to quantify microarray fluorescence. The control microarray spot quality required the following features: 50% as the minimum percentage of pixels for which the foreground intensity was greater than the background intensity + 2 S.D. values; 80 pixels as the minimum number of pixels; absence of saturated pixels. Median values for the foreground and background of each channel were normalized using the MIDAW Web tool (28). A -fold change cut-off of 1.5 filtered by variance coefficient was used to select differentially expressed genes. Genes within each group were examined for functional enrichment using Gene Ontology categories.

Pathway Analysis—Normalized transcriptional data were analyzed with Eu.Gene Analyzer 5.1 (29), using Fisher's exact

[3] The abbreviations used are: BTAa, bicycles from tartaric acid and amino acids; MIC, minimum inhibitory concentration; FET, Fisher's exact test; YPD, yeast peptone dextrose; ROS, reactive oxygen species.

test (FET) and then visualized with T-MEV 4.4 (30). This approach describes each pathway as up- or down-regulated, considering the relative number of up- or down-regulated genes annotated to that pathway and the result of the FET, false discovery rate-corrected, for the same pathway. In our analysis, we included yeast pathways from the KEGG (31), Reactome (32), and YOUNG (lists of target genes for known transcription factors) (33) databases. Transcriptional data of deletion mutant strains were obtained from the Rosetta compendium (34). Clustering of pathway-based analysis of microarray data was performed according to the procedure described in Ref. 35.

Fluorescence Microscopy—After 4 h of treatment with **089** at 0.2 mM concentration, or without it as a control, cultured cells were resuspended at 1×10^6 cells/ml in 10 mM HEPES buffer, pH 7.4, containing 5% glucose. Rhodamine B hexyl ester (Molecular Probes) was added to a final concentration of 100 nM. After 15–30 min of incubation, the mitochondrial membrane potential was visualized by fluorescence microscopy (excitation λ at 555 nm, green; emission λ at 579 nm, red). An equal aliquot of cells was treated with dihydrorhodamine 123 (Molecular Probes) to analyze endogenous reactive oxygen species (ROS) production, observed after 60 min of incubation (excitation λ at 505 nm, blue; emission λ at 534 nm, green). Each aliquot was treated with Calcofluor White (M2R) (blue) to show the cell wall in order to count total cells.

RESULTS

Selection of the Panel of Strains—Several easily detectable phenotypes in the yeast cell are related to growth rate, respiratory metabolism, and cell wall-multidrug resistance. The panel of strains of the budding yeast we have selected encompasses *S. cerevisiae* wild type for respiratory function and multidrug resistance, two laboratory strains, W303 and FY2609, and one wine strain, 0117. We probed the effect of the molecules on respiration by using strains altered in the respiratory function, BY4742 and FY2607, that harbor a mutation caused by a transposon in the *HAP1* coding sequence that reduces Hap1p function by 75% (4, 17–19). This mutation was studied alone and in combination with other deficiencies in genes involved in cell wall and multidrug resistance (Δ*erg6*, Δ*snq2*, and Δ*pdr3*). Erg6p is a sterol 24C-methyl transferase, which is involved in the synthesis of ergosterol; Snq2p is a drug efflux pump belonging to the family of the ATP-binding cassette transporters, conferring resistance to many drugs and oxygen radicals; Pdr3p is a zinc finger protein, a transcriptional coactivator (in association with Pdr1p) of genes encoding ATP-binding cassette transporters.

First Level Assays—The effects of 104 compounds, composing a preconstituted library, each at 0.1 mM concentration, were initially tested on W303 and 0117 wild-type strains. These molecules (supplemental Table 1), which are both secondary and tertiary amides based on the 6,8-dioxa-3-azabicyclo[3.2.1]-octane scaffold (Table 1), were synthesized as described previously (22–26).

Because the two strains showed the same fitness behavior after treatment with the molecules, indicating that the higher membrane permeability associated with 0117 did not affect the drug effects, we referred in the other assays to W303 only. One of the tested compounds induced a growth rate increase between 10 and 20%, whereas 22 compounds resulted in a decrease between 10 and 20%, and six molecules resulted in a decrease between 20 and 50% of growth rate (supplemental Table 2). Thus, higher concentrations (1 and 0.5 mM) of the compounds inducing more than 10% growth decrease at a concentration of 0.1 mM were tested. Effects of intermediate concentration (0.4, 0.3, and 0.2 mM) of 16 molecules inducing a more than 80% growth decrease in W303 were then investigated (Table 2).

To gain insight into the effect of the molecules on fundamental cellular functions, second level assays were conceived by testing the effect of the selected molecules on a panel of deletion mutant strains constructed in the BY4742 genetic background, compared with the parental strain. Notably, molecules that were selected because of their ability to negatively affect the growth rate of W303 and 0117 mostly induced an increase or only a weak decrease in growth rate in BY4742. This observation suggests that the different genetic backgrounds of these two strains influenced the results. W303 and BY4742 are highly genetically similar, although one of the most striking differences is the presence of a transposon insertion in the coding region of the *HAP1* gene in the BY4742 strain. The alteration in Hap1p function is known to reduce BY4742 respiratory ability (4, 17–19). The effect of the 16 compounds that induced a decrease between 10 and 20% in the wild-type genetic context was further tested on BY4742Δ*erg6*, BY4742Δ*snq2*, and BY4742Δ*pdr3* strains at a concentration of 0.3 mM, which is the minimum concentration that induced an effect on the wild-type strain (Fig. 1). Five of the compounds tested, **011**, **012**, **018**, **022** and **028**, decreased the growth rate of W303, whereas they showed no effects on BY4742 and an increase in BY4742Δ*snq2* and BY4742Δ*erg6* mutant strains. This effect can be attributed to an increase in the intracellular/cytoplasmic concentration of the molecule, due to a defect in the efflux activity (deletion of *SNQ2*) or to a higher membrane permeability (deletion of *ERG6*). Four of the molecules tested were able to increase the growth rate of BY4742. Specifically, **066** and **067** exerted the same effect even on Pdr3p and Snq2p; **038** and **053** induced an increase in growth rate even on Pdr3p, Snq2p, and Erg6p. Further assays on **089**, which was identified as the molecule inducing the most intense cell growth decrease (more than 80%), showed that after 18 h of treatment at 0.3 mM concentration, the variation in OD_{650} value of the culture of BY4742Δ*erg6* became negative due to cell death, confirmed by microscopic observation with LIVE/DEAD (live cells converting the green fluorescent intracellular staining FUN1 dye into red fluorescent intravacuolar structures) and methylene blue (dead cells turning blue) assays as well as the presence of cellular debris.

Relationship between Molecular Structure and Biological Effect—The screening conducted in this study was carried out by treating a whole organism with small molecules. Analysis of the observed effects provided information on the connection between the molecular structure and the ability to perturb the growth rate of treated cells, regardless of the target receptor of each molecule. The class of molecules having the general structure III, as shown in Table 1 (**106**, **107**, **108**, **110**, **111**, **112**, **113**, and **114**) induced a growth rate decrease only if the molecule

TABLE 1

Scheme of tested compounds

The tested library is composed of bicyclic peptidomimetics, BTAa (bicycles from tartaric acid and amino acids), which present all of the combinations of the R groups with the three selected scaffolds. Bn, benzyl; Bzh, benzhydryl; s-Bu, *sec*-butyl; TBDMS, *tert*-butyldimethylsilyl; *p*-NO_2-Ph, *p*-nitrophenyl; TFE, trifluoroethyl; *n*Pr, propyl; Cyp, cyclopropyl; Prg, propargyl; *n*Bu, butyl; iAm, isoamyl; Hex, hexyl; Cyh, cyclohexyl; MBn, (*S*)-α-methylbenzyl; *i*Pr, isopropyl; *t*Bu, *tert*-butyl.

	R^1	R^2	R^3	$R^{4'}$	$R^{4''}$
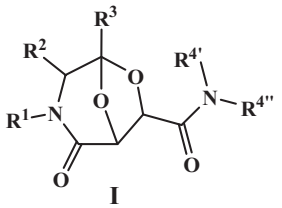 I 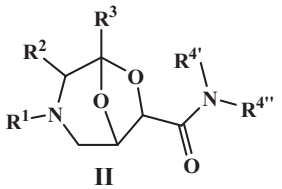 II 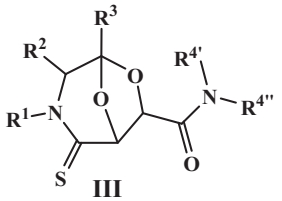 III	Bn, Bzh	H, Me, s-Bu, Bn, Ph, CH_2OBn, $CH_2OTBDMS$	H, Ph, *p*-NO_2-Ph	H, Me, TFE, *n*Pr, Cyp, Prg, *n*Bu, *i*Am, Hex, Cyh, Bn, MBn, 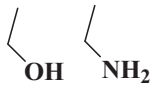	H
				Me, Et, *i*Pr, *t*Bu	Me, Et, *i*PR, *t*Bu
				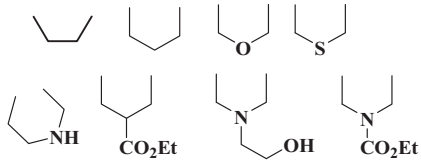	
				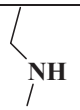	Me

had a secondary amine as the R^4 group. The molecules containing a leucine isostere as the R^1 group (**119**, **120**, **123**, and **124**) did not induce effects in any case. Phenotypic effects of compounds having an ethyl group at R^4, (**020**, **024**, **025**, **042**, **049**, **057**, **072**, **075**, **076**, **089**, and **090**) suggested that 1) the presence of a protic donor group (resulting in R^4 hydroxyethyl residue), which in some cases was connected to higher cell growth rate, and 2) the substitution of the methyl group with CF_3 at the second position of the ethylamine was associated with a higher growth decrease, not attributable to the steric hindrance of fluorine (similar to hydrogen) but to the ability to form polar interactions. The ability of molecules having the general structure I, as shown in Table 1 (**056**, **057**, **058**, **059**, **060**, **061**, **066**, **067**, **068**, **069**, **070**, and **071**), to induce a biological effect was associated with the steric hindrance of the R^4 group; the lower the steric hindrance, the higher the biological effect, decreasing up to 50% in the presence of a bulkier group. On the contrary, the opposite correlation was evident in molecules possessing the scaffold II, as shown in Table 1 (**001**, **002**, **004**, **005**, **008**, **009**, **010**, **011**, **012**, **013**, **014**, **015**, **016**, and **018**), thus suggesting two different targets for the two compound classes. By comparing **089** with other molecules of the library that differed in some functional groups, a drastic decrease in the ability to induce a biological effect was seen to be due to the lack of the carbonyl group embedded in the bicycle, the benzhydryl group substitution with a benzyl group, and the lipophilic R^4 chain elongation.

Second Level Assays—The MIC of **089** on W303 and BY4742 wild-type strains was determined (supplemental Fig. 1). Both strains were characterized by a MIC of 1 mM, but the EC_{50} values, which were 0.25 mM for W303 strain and 0.38 mM for BY4742 strain, were more interesting. The survival rate of the strains W303, BY4742, BY4742Δ*erg6*, BY4742Δ*snq2*, and BY4742Δ*pdr3* after a 2- and 4-h treatment with different concentrations of **089** (1, 0.5, 0.2, and 0.1 mM and control) was evaluated. The results of this assay (Fig. 2) showed that at higher concentrations, the molecule induced steady effects in each strain even at the early time points. Lower concentrations (up to 0.1 mM in the 2-h treatments and up to 0.2 mM in the 4-h treatments) induced a survival percentage decrease only for W303, thus confirming the MIC results. Each strain showed almost the same higher survival decrease at 0.5 mM concentration of **089** (nearly 30% in the 2-h treatment, around 10% in the 4-h treatment). By contrast, BY4742 revealed itself to be the most resistant to the treatment, as previously observed. The 4-h exposure to **089** with a concentration of 1 mM triggered the same effects on all of the tested strains, including BY4742. The concentration of **089** inhibiting the growth of deletion mutant strains induced a minor effect on BY4742, probably due to different respiratory ability.

Because the two wild-type tested strains, BY4742 and W303, had a different genetic background, we further investigated the role of *HAP1* using FY2609 (*HAP1*) and FY2607 (*hap1T*) as two

TABLE 2

Structures and effects of compounds selected from the first level assay

Molecules were selected because of their ability to induce (at a concentration of 0.5 mM) a growth decrease more intense than 80% in W303 strain with respect to the growth rate of the untreated strain. Numbers used to designate molecules refer to the position in the library. The effect of each molecule was calculated as percentage variation of the OD_{650} of a cell culture grown on YPD (pH 4.8) supplemented with molecule at various concentrations in comparison with a cell culture grown on YPD (pH 4.8). ----, variation ≥ |80|%; ---, variation ≥ |50|%; --, variation ≥ |20|%; -, variation ≥ |10|%; =, no effect.

Name	Structure	Molecule concentration (mM)					
		1	0.5	0.4	0.3	0.2	0.1
008	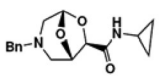	----	----	--	--	-	-
011	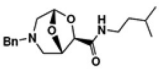	----	----	--	-	-	-
012	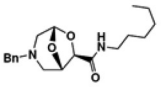	----	----	--	-	=	-
014	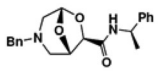	----	----	--	--	=	-
038	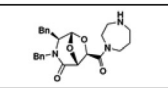	----	----	--	--	=	-
042	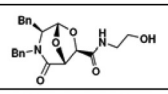	----	----	--	=	=	=
049	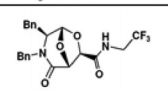	----	----	--	---	--	-
050	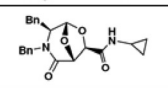	----	----	--	-	--	-
066	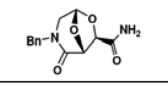	----	----	-	=	=	=
071	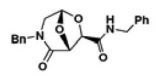	----	----	--	-	=	-
076	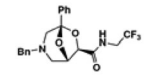	----	----	--	--	-	-
089	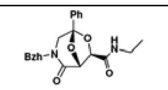	----	----	----	----	--	-
124	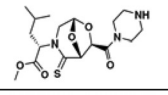	----	----	--	---	=	-
135	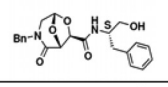	----	----	--	--	=	-
136	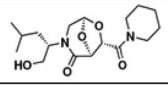	----	----	--	--	=	-
137	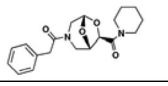	----	----	-	-	=	=

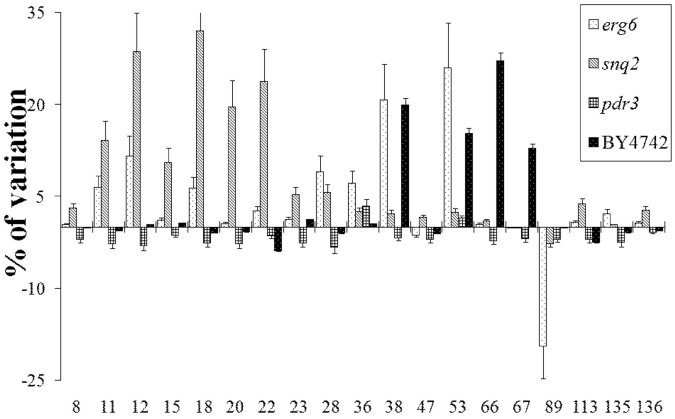

FIGURE 1. **Treatment effects.** Effects of molecules selected in the first level assay tested at the concentration of 0.3 mM on BY4742Δ*erg6*, BY4742Δ*snq2*, and BY4742Δ*pdr3* were compared with BY4742. The effect of each molecule was calculated as percentage variation of the OD_{650} of a cell culture grown on YPD (pH 4.8) supplemented with molecule at various concentrations compared with a cell culture grown on YPD (pH 4.8). *Numbers* used to designate molecules refer to the position in the library. *Error bars*, S.D. values obtained by three measures of the percentage of growth variation.

additional strains having similar alterations of *HAP1* in the same genetic background. The FY strains (36) have a similar pedigree and genetic background as the BY series strains, all being derivatives of S288c; therefore, the results observed in FY2607 can be reasonably generalized to BY4742. We treated the FY strains with **089** at 0.3 mM concentration. We observed an inhibition rate of 7% for FY2607 *hap1T* and of 8.9% for FY2609 *HAP1*, and this difference was statistically significant ($p < 0.05$). These results confirmed the *HAP1*-associated trend highlighted in the comparison between BY4742 and W303. Specifically, compound **089** elicits stronger inhibiting effects in the presence of the wild-type *HAP1* gene. To further investigate the role of the *HAP1* gene in combination with the other mutations studied, we are planning to introduce the wild-type allele into the BY4742 strain and into the three knock-out strains, BYΔ*erg6*, BYΔ*snq2*, and BYΔ*pdr3*.

Transcriptional Analysis—Transcriptional analysis following the treatment with **089** at 0.2 mM concentration was carried out on deletion mutant strains that in former assays showed higher sensitivity to the treatment (BY4742Δ*erg6* and BY4742Δ*snq2*) and on the parental strain (BY4742). We chose to perform the transcriptional profiling in the presence of a molecule concentration having some effects on cell viability but allowing survival of at least 50% of treated populations, as determined by EC_{50} evaluation. We focused on the laboratory type strains because a large quantity of publicly available data make this genetic background the most suitable for further comparisons of transcriptional profiles obtained in this study with those present in public databases. We analyzed the lists of differentially expressed genes obtained, applying 1.5 as the -fold change threshold. The two deletion mutants showed an overexpression of genes coding mitochondrial proteins or genes involved in respiration and in response to oxidative stress, in contrast to BY4742. This strain also showed down-regulation of genes encoding some mitochondrial F_1F_0-ATP synthase subunits (*ATP1*, *ATP2*, *ATP3*, *ATP4*, and *ATP16*). The deleted strains showed increased expression

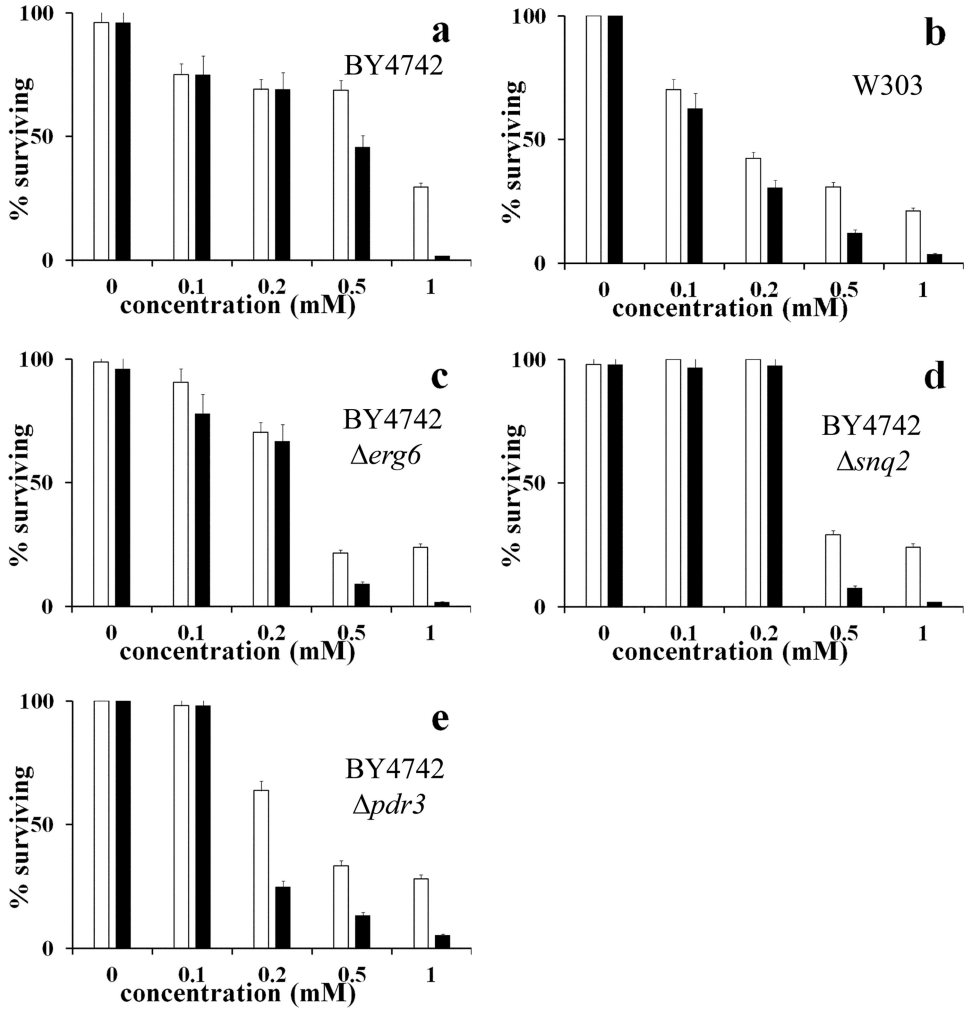

FIGURE 2. **Survival rate after treatment with 089.** *a*, survival rate of BY4742 strain; *b*, survival rate of W303 strain; *c*, survival rate of BY4742Δ*erg6* strain; *d*, survival rate of BY4742Δ*snq2* strain; *e*, survival rate of BY4742Δ*pdr3* strain. *White*, 2-h treatment with **089**; *black*, 4-h treatment. The yeast strain survival rates were calculated as the number of live cells (by LIVE/DEAD and methylene blue assays) per 100 divided by the total number of the same strain untreated. Values indicate the mean of two measurements, and *error bars* indicate the corresponding S.D. values.

of some of the mitochondrial electron transport chain complexes, such as nuclear genes coding for subunits of the cytochrome *c* oxidase (*COX9*, *COX5A*, *COX6*, and *COX13*) and of the succinate dehydrogenase (*SDH1*, *SDH3*, and *SDH4*) and a mitochondrial porin (*POR1*). When comparing genes undergoing a variation in expression levels exclusively in the deleted strains, a large majority of genes coding mitochondrial proteins (*NDE2*, *LSC2*, *ACS1*, *PPA2*, *CIT2*, *CIT3*, etc.) or involved in respiration (*ETR1*, *QCR7*, *LSC2*, *MBR1*, and *PPA2*) were detectable, and those genes were all overexpressed. The macromolecular complex disassembly (genes involved are *SSB1*, *RSC3*, *TPA1*, *YGL120C*, and *RSC58*) was up-regulated in BY4742 but down-regulated in BY4742Δ*snq2*, thus showing no significant variation in BY4742Δ*erg6.* These results can be ascribed to an increase in the intracellular concentration of the molecule, depending on a decrease of membrane rigidity in the case of the Δ*erg6* mutant or on reduction of intracellular levels of the molecule by extrusion in the case of the Δ*snq2* mutant. The higher the intracellular concentration, the higher are the drug effects. Because the two deleted strains herein investigated have the same genetic background as BY4742, the observation of overexpression of genes involved in respiration and response to oxidative stress only in the deleted strains suggests that the intracellular concentration of the molecule in the wild-type strain is reduced by active export mechanisms. As a consequence, the effects are more pronounced in deletant strains. Every strain showed an up-regulation of genes involved in telomere maintenance and organization and in homeostatic processes (*YRF1-1*, *YRF1-2*, *YRF1-3*, *YRF1-4*, *YRF1-5*, *YRF1-6*, and *YRF1-7*), showing instead a down-regulation of genes involved in protein folding and protein targeting to membrane and to endoplasmic reticulum (*SSA1*, *SSA4*, *SSE1*, *SSE2*, *YDJ1*, *HSP82*, and *KAR2*), thus indicating that **089** induces cellular damage, as indicated also by the up-regulation of telomere maintenance and organization.

Pathway Analysis—Pathway analysis was used to assign a probability of alteration in selected pathways by using the FET *p* value as an indication of the likelihood of the involvement of a cellular compartment or of a set of biological reactions. Pathway analysis over our selected set of pathways was carried out using the FET (see "Experimental Procedures"). The Fisher's test *p* value, along with the state of regulation of each pathway (described considering the relative number of up- or down-regulated genes annotated to that pathway) indicated the likelihood of its involvement. The pathway analysis of transcriptional data confirmed the increase in respiratory deficiency, highly evident in the BY4742Δ*erg6* strain, and of anaerobic respiration, especially of the electron acceptor reaction list and electron transport chain, with an opposite trend in the wild-type strain. This result confirmed the involvement of respiratory metabolism and *HAP1* function in response to **089**, confirming *HAP1* as one of the targets.

We further used an advanced pathway approach to compare the three experiments of this study with a collection of publicly available experiments describing the effect on transcription of selective gene deletions. This approach uses pathway signatures to compare experiments at the pathway level (35). We used this approach with a chemical genetic mindset, asking which other deletion was phenocopied at a transcriptional level by **089**. If bootstrap-based clustering approaches of the pathway signatures reveal similarity between the transcriptional data of the treatment of yeast with **089** and the transcrip-

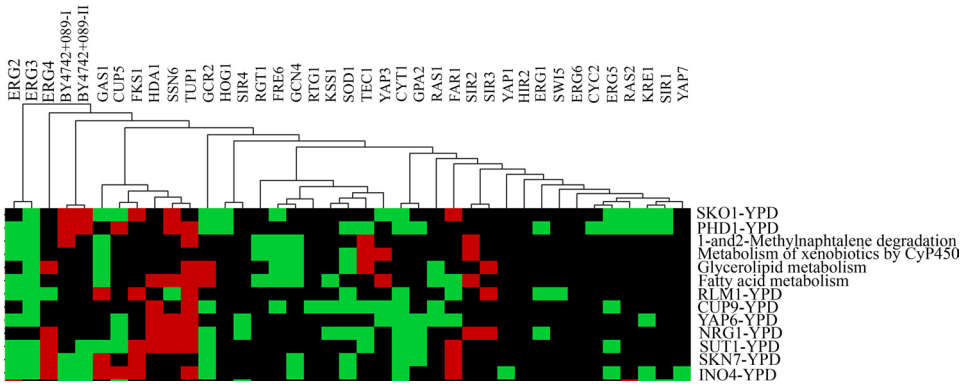

FIGURE 3. **Pathway signatures visualized with T-Mev 4.4.** Pathway signatures were obtained with Eu.Gene Analyzer 5.1, using FET and then visualized with T-MEV 4.4. This is a significant selection of the pathway analysis and the relative sample cluster of transcriptional data of the treatment of yeast with **089**. Up-regulated pathways are visualized in *red*, and down-regulated pathways are shown in *green*. Yeast pathways from the KEGG, Reactome, and YOUNG databases were included in the analysis. The YOUNG list is composed of target genes for known transcription factors.

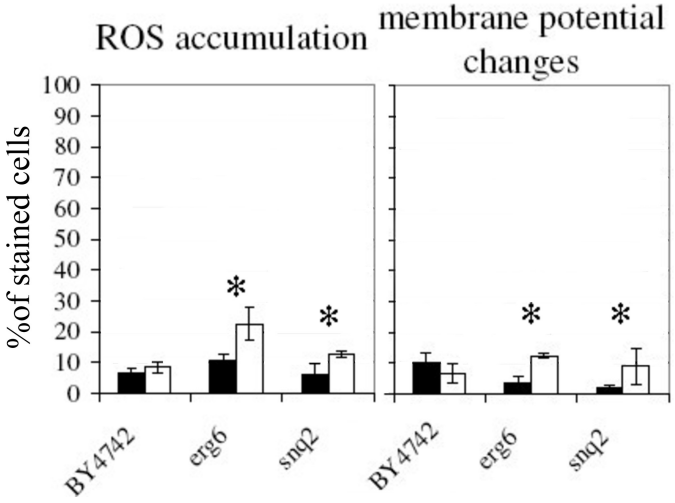

FIGURE 4. **Quantitative evaluation of ROS accumulation and mitochondria activation.** Wild-type strain cells (BY4742) and deletant strain cells (BY4742Δ*erg6* and BY4742Δ*snq2*) were treated for 4 h with **089** at 0.2 mM concentration, and then the mitochondrial membrane potential was detected by rhodamine B hexyl ester staining, and ROS accumulation was evaluated by dihydrorhodamine 123 staining. *White*, the percentage values corresponding to cells treated with **089**; *black*, the percentage values of untreated cells. Percentages were calculated as the mean of the number of stained cells over total cells in the optical field evaluated in triplicate. Student's *t* test was used to evaluate the data significance. *, $p < 0.05$. Error bars, S.D.

tional data of a group of untreated deletion yeast strains, then it is possible to hypothesize the molecular target at the pathway level. Interestingly, by this comparison, it is possible to observe a similarity between the effects of the treatment with molecule **089** and the effects of the two gene deletions Δ*erg4* and Δ*gas1* (Fig. 3). Both of these genes are involved in cell wall and membrane assembly, the first encoding C-24(28) sterol reductase, which catalyzes the final step in ergosterol biosynthesis, the latter encoding β-1,3-glucanosyltransferase, required for cell wall assembly. The treatment with **089** and the deletion of *ERG4* showed up-regulation in the metabolism of glucose, carbohydrates, and small molecules and in glycolysis and gluconeogenesis and down-regulation in the oxidative branch of the pentose phosphate pathway in methionine metabolism, methylation, and methyl donor molecule biosynthesis. The treatment with **089** and the deletion of the *GAS1* gene showed a down-regulation of the complex involved in regulating the histone gene transcription (*HIR2*).

By probing enrichment for target genes of specific transcription factors, we observed that **089** induces an overregulation of genes controlled by *CIN5*, a transcriptional factor that mediates pleiotropic drug resistance. Deletions of *ERG4* and *GAS1* have an opposite transcriptional effect on the *CIN5* targets, defining a transcriptional module as affected by this treatment. The effects induced by cell wall misassembly (even at the nuclear level) seem to be more similar to those induced by the treatment of wild-type yeast strain with **089** than those induced by cell membrane misassembly. This suggests that the molecule selected in this work targets a component of the cell wall and consequently induces oxidative stress. Given that the wall is a peculiar yeast structure not present in higher eukaryotic cells, **089** has great potential to act as a selective antifungal.

Effects of the Molecule on Mitochondria—In addition to showing effects on mitochondria, transcriptional pathway analysis highlighted that the treatment with **089** induces up-regulation of the breakdown of hydrogen peroxide to water and molecular oxygen and of *SKN7*, a transcriptional factor required for optimal induction of heat-shock genes in response to oxidative stress. We then investigated the effects of **089** on ROS accumulation and mitochondrial membrane potential activation. Deletant strains BY4742Δ*erg6* and BY4742Δ*snq2* treated for 4 h with **089** at 0.2 mM concentration, after staining with dihydrorhodamine 123, showed twice as much ROS (22 and 12%, respectively) as the ROS of deletant untreated cultures (10 and 6%, respectively) (Fig. 4), confirming transcriptional analysis indications. The wild-type strain BY4742 did not show any variation in ROS accumulation after treatment with **089**.

The profile observed in ROS accumulation was confirmed when evaluating mitochondrial activation. Cells of the deletant strains stained with rhodamine B hexyl ester showed a 3-fold increase in mitochondrial membrane potential activation (12 and 9%), compared with untreated cells (4 and 2%), whereas the wild-type strain mitochondrial activation level did not change in either treated or untreated cells (Fig. 4).

DISCUSSION

Yeast genetics, cell biology, and molecular genetics have benefited enormously from the presence of a well characterized set of strains derived from S288c genetic background. S288c is profoundly different from other strains of the *S. cerevisiae* genus (37–39). When using yeast in chemical genetics studies, the extent to which a phenotype induced by a molecule is dependent on the genetic background of the S288c derivatives is yet to be fully understood. The results presented herein demonstrate

TABLE 3

Strains tested in assays with 089

The inhibition rate assay refers to the treatment with **089** at 0.3 mM concentration, whereas the transcriptional analysis, ROS production, and mitochondrial membrane activation evaluations have been done using **089** at 0.2 mM concentration. Inhibition rates were calculated as the percentage of inhibition compared with the untreated culture. The ROS production and mitochondrial membrane activation percentage values were calculated as the mean of the number of stained cells over total cells on the optical field. NT, not treated.

Strain	HAP1 type	Inhibition rate	MIC	EC_{50}	Transcriptional analysis	ROS production		Mitochondrial membrane activation	
						089	NT	089	NT
		%	mM	mM		%	%	%	%
W303	*HAP1*	83	1	0.25					
BY4742	*hap1T*	0.3	1	0.38	Yes	0	0	0	0
BY4742Δ*erg6*	*hap1T*	19.3			Yes	22	10	12	4
BY4742Δ*snq2*	*hap1T*	2.6			Yes	12	6	9	2
BY4742Δ*pdr3*	*hap1T*	1.9							
FY2607	*hap1T*	7							
FY2609	*HAP1*	8.9							

the influence of a functional *HAP1* gene in the performance of *S. cerevisiae* as a model system and the importance of using a panel of strains to investigate the effects of a library of bioactive molecules. The set of strains used in this work significantly broadens the ability to dissect the biological effects of a selected family of molecules, thus circumventing the limitations of the laboratory strain S288c. Our results show how a combined use of the proposed panel of gene deletion strains with alterations in the respiratory function or multidrug resistance-cell wall function can ascribe the biological function of a molecule to a specific set of biological processes, paving the way to more insightful investigations. The selected peptidomimetic **089** induces more severe effects on the wild-type W303 strain, having a functional *HAP1* gene, than on the laboratory BY4742 strain, having almost the same genetic background as W303 but the mutated *HAP1* gene, thus giving an indication of an involvement of the respiratory metabolism in response to **089** perturbation. This hypothesis is confirmed even by the *HAP1*-associated trend of the molecule effects on FY strains. The strain FY2609 (*HAP1*) showed greater inhibition than FY2607 (*hap1T*). Nevertheless, the intensity effect is weaker on FY strains than on the W303 strain, indicating that a *HAP1*-mediated increase in the respiratory metabolism alters the effects of **089** in a genetic background-associated function. It is evident that a number of other genetic differences between the strains could have epistatic effects on this phenotype. Overall, considering the wide range and differences of effects exerted by the treatment with **089** on different strains, the genetic background of the strain used for the screening again turns out to be of extreme relevance when evaluating the biological effects of small molecules (Table 3).

The use of a pool of strains bearing deletions of genes involved in membrane assembly or function enables the identification of effects that could be concealed by the membrane permeation incapability of the molecule. This is suggested by the opposite effect of **089** on yeast growing rate, which decreases for deletant strains but increases for the wild-type strain. Transcriptional analysis indicates the presence of an important stress condition that occurs more prominently in the deletion mutant strains, a variation that can be ascribed to a higher ability of the molecule to permeate the cellular or mitochondrial membrane or to remain in the cell cytoplasm. The activity of **089** in inducing an increase in respiratory deficiency and anaerobic respiration is confirmed by pathway analysis of transcriptional data, thus corroborating the *HAP1* as one of the targets. The induction of oxidative stress at the mitochondrial level is confirmed by an increase in ROS accumulation and mitochondrial membrane activation level.

The application of the novel pathway-based approach (35) to compare **089** effects at the transcriptional level with those of a pool of gene deletions is a powerful *in silico* simulation that identifies response trends to different stimuli (the former a molecule, the latter a gene function loss). Accordingly, we identified a similar trend between the treatment with **089** and the deletion of *GAS1* and *ERG4*, the former stricter and the latter weaker, leading to localization of the first molecular target at the cell wall level, with oxidative stress being a secondary effect. The cell wall is a peculiar yeast structure; hence, it is an excellent target for selective antifungal drugs.

The pathway signature-based approach used here holds the promise of enabling the classification of bioactive molecules based on their transcriptional pathway signatures and the assessment of similarity of the effects of different molecules based on the pathway profile. By taking advantage of all of these findings, it was possible to identify **089** as a potential selective antifungal.

Model organisms that have evolved in permissive laboratory conditions may introduce a bias into the assessment of biological functions of a molecule, derived from the accumulation of genetic defects in laboratory strains (such as the improper respiratory metabolism). When using yeast to learn fundamental lessons about cell biology or the mechanism of action of a molecule, often to be generalized to mammalian cells, it is fundamental to assess to what extent the observed phenotype can be generalized to other yeasts of the same species. In this study, the use of a panel of different strains has been fundamental to the analysis of the relationship between the activity and the structure of the whole peptidomimetic library and cell function, thus providing important insights for optimization of its activity.

Acknowledgments—We are grateful to Dan Spatt for supplying the FY strains, to Luca Beltrame for helpful discussion on pathways analysis, and to Mary Forrest for linguistic editing. We also thank Fondazione Giuseppe Tommasello Organizzazione Non Lucrativa di Utilità Sociale.

REFERENCES

1. Verkman, A. S. (2004) *Am. J. Physiol. Cell Physiol.* **286,** C465–474
2. Kawasumi, M., and Nghiem, P. (2007) *J. Invest. Dermatol.* **127,** 1577–1584
3. Dean, P. M. (2007) *Mol. Biotechnol.* **37,** 237–245
4. Hoon, S., St Onge, R. P., Giaever, G., and Nislow, C. (2008) *Trends Pharmacol. Sci.* **29,** 499–504
5. Stockwell, B. R. (2000) *Trends Biotechnol.* **18,** 449–455
6. Giaever, G. (2003) *Trends Pharmacol. Sci.* **24,** 444–446
7. Spring, D. R. (2005) *Chem. Soc. Rev.* **34,** 472–482
8. Zheng, X. F., and Chan, T. F. (2002) *Curr. Issues Mol. Biol.* **4,** 33–43
9. Huang, J., Zhu, H., Haggarty, S. J., Spring, D. R., Hwang, H., Jin, F., Snyder, M., and Schreiber, S. L. (2004) *Proc. Natl. Acad. Sci. U.S.A.* **101,** 16594–16599
10. Lo, M. M., Neumann, C. S., Nagayama, S., Perlstein, E. O., and Schreiber, S. L. (2004) *J Am. Chem. Soc.* **126,** 16077–16086
11. Resnick, M. A., and Cox, B. S. (2000) *Mutat. Res.* **451,** 1–11
12. Brenner, C. (2004) *Genome Biol.* **5,** 240
13. Giaever, G., Flaherty, P., Kumm, J., Proctor, M., Nislow, C., Jaramillo, D. F., Chu, A. M., Jordan, M. I., Arkin, A. P., and Davis, R. W. (2004) *Proc. Natl. Acad. Sci. U.S.A.* **101,** 793–798
14. Lum, P. Y., Armour, C. D., Stepaniants, S. B., Cavet, G., Wolf, M. K., Butler, J. S., Hinshaw, J. C., Garnier, P., Prestwich, G. D., Leonardson, A., Garrett-Engele, P., Rush, C. M., Bard, M., Schimmack, G., Phillips, J. W., Roberts, C. J., and Shoemaker, D. D. (2004) *Cell* **116,** 121–137
15. Parsons, A. B., Brost, R. L., Ding, H., Li, Z., Zhang, C., Sheikh, B., Brown, G. W., Kane, P. M., Hughes, T. R., and Boone, C. (2004) *Nat. Biotechnol.* **22,** 62–69
16. Parsons, A. B., Lopez, A., Givoni, I. E., Williams, D. E., Gray, C. A., Porter, J., Chua, G., Sopko, R., Brost, R. L., Ho, C. H., Wang, J., Ketela, T., Brenner, C., Brill, J. A., Fernandez, G. E., Lorenz, T. C., Payne, G. S., Ishihara, S., Ohya, Y., Andrews, B., Hughes, T. R., Frey, B. J., Graham, T. R., Andersen, R. J., and Boone, C. (2006) *Cell* **126,** 611–625
17. Brem, R. B., Yvert, G., Clinton, R., and Kruglyak, L. (2002) *Science* **296,** 752–755
18. Gaisne, M., Bécam, A. M., Verdière, J., and Herbert, C. J. (1999) *Curr. Genet.* **36,** 195–200
19. Tamura, K., Gu, Y., Wang, Q., Yamada, T., Ito, K., and Shimoi, H. (2004) *J. Biosci. Bioeng.* **98,** 159–166
20. Gante, J. (1994) *Angew. Chem. Int. Ed. Engl.* **33,** 1699–1720
21. Burke, M. D., and Schreiber, S. L. (2004) *Angew. Chem. Int. Ed. Engl.* **43,** 46–58
22. Guarna, A., Bucelli, I., Machetti, F., Menchi, G., Occhiato, E. G., Scarpi, D., and Trabocchi, A. (2002) *Tetrahedron* **58,** 9865–9870
23. Guarna, A., Guidi, A., Machetti, F., Menchi, G., Occhiato, E. G., Scarpi, D., Sisi, S., and Trabocchi, A. (1999) *J. Org. Chem.* **64,** 7347–7364
24. Machetti, F., Bucelli, I., Indiani, G., Kappe, C. O., and Guarna, A. (2007) *J. Comb. Chem.* **9,** 454–461
25. Trabocchi, A., Menchi, G., Guarna, F., Machetti, F., Scarpi, D., and Guarna, A. (2006) *Synlett* **3,** 331–353
26. Trabocchi, A., Occhiato, E. G., Potenza, D., and Guarna, A. (2002) *J. Org. Chem.* **67,** 7483–7492
27. Landry, C. R., Oh, J., Hartl, D. L., and Cavalieri, D. (2006) *Gene.* **366,** 343–351
28. Romualdi, C., Vitulo, N., Del Favero, M., and Lanfranchi, G. (2005) *Nucleic. Acids. Res.* **33,** W644–649
29. Cavalieri, D., Castagnini, C., Toti, S., Maciag, K., Kelder, T., Gambineri, L., Angioli, S., and Dolara, P. (2007) *Bioinformatics* **23,** 2631–2632
30. Saeed, A. I., Sharov, V., White, J., Li, J., Liang, W., Bhagabati, N., Braisted, J., Klapa, M., Currier, T., Thiagarajan, M., Sturn, A., Snuffin, M., Rezantsev, A., Popov, D., Ryltsov, A., Kostukovich, E., Borisovsky, I., Liu, Z., Vinsavich, A., Trush, V., and Quackenbush, J. (2003) *BioTechniques* **34,** 374–378
31. Kanehisa, M., Goto, S., Hattori, M., Aoki-Kinoshita, K. F., Itoh, M., Kawashima, S., Katayama, T., Araki, M., and Hirakawa, M. (2006) *Nucleic Acids Res.* **34,** D354–357
32. Joshi-Tope, G., Gillespie, M., Vastrik, I., D'Eustachio, P., Schmidt, E., de Bono, B., Jassal, B., Gopinath, G. R., Wu, G. R., Matthews, L., Lewis, S., Birney, E., and Stein, L. (2005) *Nucleic Acids Res.* **33,** D428–D432
33. Lee, T. I., Rinaldi, N. J., Robert, F., Odom, D. T., Bar-Joseph, Z., Gerber, G. K., Hannett, N. M., Harbison, C. T., Thompson, C. M., Simon, I., Zeitlinger, J., Jennings, E. G., Murray, H. L., Gordon, D. B., Ren, B., Wyrick, J. J., Tagne, J. B., Volkert, T. L., Fraenkel, E., Gifford, D. K., and Young, R. A. (2002) *Science* **298,** 799–804
34. Hughes, T. R., Marton, M. J., Jones, A. R., Roberts, C. J., Stoughton, R., Armour, C. D., Bennett, H. A., Coffey, E., Dai, H., He, Y. D., Kidd, M. J., King, A. M., Meyer, M. R., Slade, D., Lum, P. Y., Stepaniants, S. B., Shoemaker, D. D., Gachotte, D., Chakraburtty, K., Simon, J., Bard, M., and Friend, S. H. (2000) *Cell* **102,** 109–126
35. Beltrame, L., Rizzetto, L., Paola, R., Rocca-Serra, P., Gambineri, L., Battaglia, C., and Cavalieri, D. (2009) *PLoS One* **4,** e4128
36. Hickman, M. J., and Winston, F. (2007) *Mol. Cell. Biol.* **27,** 7414–7424
37. Liti, G., Carter, D. M., Moses, A. M., Warringer, J., Parts, L., James, S. A., Davey, R. P., Roberts, I. N., Burt, A., Koufopanou, V., Tsai, I. J., Bergman, C. M., Bensasson, D., O'Kelly, M. J., van Oudenaarden, A., Barton, D. B., Bailes, E., Nguyen, A. N., Jones, M., Quail, M. A., Goodhead, I., Sims, S., Smith, F., Blomberg, A., Durbin, R., and Louis, E. J. (2009) *Nature* **458,** 337–341
38. Schacherer, J., Shapiro, J. A., Ruderfer, D. M., and Kruglyak, L. (2009) *Nature* **458,** 342–345
39. Zhu, J., Zhang, B., Smith, E. N., Drees, B., Brem, R. B., Kruglyak, L., Bumgarner, R. E., and Schadt, E. E. (2008) *Nat. Genet.* **40,** 854–861

A Systems Biology Approach to Dissection of the Effects of Small Bicyclic Peptidomimetics on a Panel of *Saccharomyces cerevisiae* Mutants

Irene Stefanini, Andrea Trabocchi, Emmanuela Marchi, Antonio Guarna and Duccio Cavalieri

J. Biol. Chem. 2010, 285:23477-23485.
doi: 10.1074/jbc.M110.125153 originally published online May 25, 2010
